Stem Cell Research 38 (2019) 101480

Contents lists available at ScienceDirect

Stem Cell Research

journal homepage: www.elsevier.com/locate/scr

Lab resource: Stem Cell Line

Production and characterization of human induced pluripotent stem cells (iPSC) CSSi007-A (4383) from Joubert Syndrome

Filomena Altieri[a], Angela D'Anzi[a], Francesco Martello[a], Silvia Tardivo[b], Iolanda Spasari[c], Daniela Ferrari[d], Laura Bernardini[c], Giuseppe Lamorte[c], Gianluigi Mazzoccoli[e], Enza Maria Valente[b,f], Angelo Luigi Vescovi[a,d], Jessica Rosati[a,*]

[a] Fondazione IRCCS Casa Sollievo della Sofferenza, Cellular Reprogramming Unit, Viale dei Cappuccini, 71013 San Giovanni Rotondo, Foggia, Italy
[b] Neurogenetics Unit, IRCCS Santa Lucia Foundation, Rome 00143, Italy
[c] Fondazione IRCCS Casa Sollievo della Sofferenza, Medical Genetics Unit, Viale dei Cappuccini, 71013 San Giovanni Rotondo, Foggia, Italy
[d] Biotechnology and Bioscience Department, Bicocca University, Piazza della Scienza 2, 20126 Milan, Italy
[e] IRCCS Casa Sollievo della Sofferenza, Division of Internal Medicine and Chronobiology Unit, Viale dei Cappuccini, 71013 San Giovanni Rotondo, Foggia, Italy
[f] Department of Molecular Medicine, University of Pavia, via Forlanini 14, 27100 Pavia, Italy

A B S T R A C T

Joubert syndrome (JS) is an autosomal recessive neurodevelopmental disorder, characterized by congenital cerebellar and brainstem defects, belonging to the group of disorders known as ciliopathies, which are caused by mutations in genes encoding proteins of the primary cilium and basal body. Human induced pluripotent stem cells (hiPSCs) from a patient carrying a homozygous missense mutation (c.2168G > A) in AHI1, the first gene to be associated with JS, were produced using a virus-free protocol.

Resource table.

Unique stem cell line identifier	CSSi007-A (4383)
Alternative name(s) of stem cell line	*Joub07 cl1*
Institution	IRCCS Casa Sollievo della Sofferenza
Contact information of distributor	*Jessica ROSATIj.rosati@css-mendel.it*
Type of cell line	*iPSC*
Origin	*Human*
Additional origin info	*Applicable for human iPSC* *Age: 27 yrs* *Sex: Male* *Ethnicity if known: Caucasian/Italian*
Cell Source	*Dermal Fibroblasts*
Method of reprogramming	*Non integrating episomal vectors*
Genetic Modification	*NO*
Type of Modification	*N/A*
Associated disease	*Joubert Syndrome*
Gene/locus	(*AHI1*):c.2168G > A/6q23.3
Method of modification	*N/A*
Name of transgene or resistance	*N/A*
Inducible/constitutive system	*N/A*
Date archived/stock date	*09/01/2015*
Cell line repository/bank	*N/A*
Ethical approval	*Casa Sollievo della Sofferenza Ethical Committee, approval number: 2292/DS*

Resource utility

Joubert Syndrome is a rare, genetically heterogeneous disorder whose complexity makes it difficult to associate phenotype to genotype. The derivation of induced pluripotent cells (iPSCs) from individuals suffering from JS offers the possibility of studying this multi-organ disease *in vitro*, differentiating the iPSCs into the various cell types that are affected.

Resource details

The distinctive hallmark of Joubert Syndrome (JS) is the "molar tooth sign" (MTS), a complex midbrain-hindbrain malformation visible on brain imaging. The phenotypic presentation is extremely variable. The core neurological features include developmental delay, breathing abnormalities in the neonatal period, hypotonia, abnormal eye movements, ataxia and intellectual disability; these can be variably associated to defects in other organs, such as the retina, kidney and liver. One causative gene of JS is the Abelson helper integration site 1 (*AHI1*)

* Corresponding author.
E-mail address: j.rosati@css-mendel.it (J. Rosati).

https://doi.org/10.1016/j.scr.2019.101480
Received 26 February 2019; Received in revised form 21 May 2019; Accepted 1 June 2019
Available online 05 June 2019

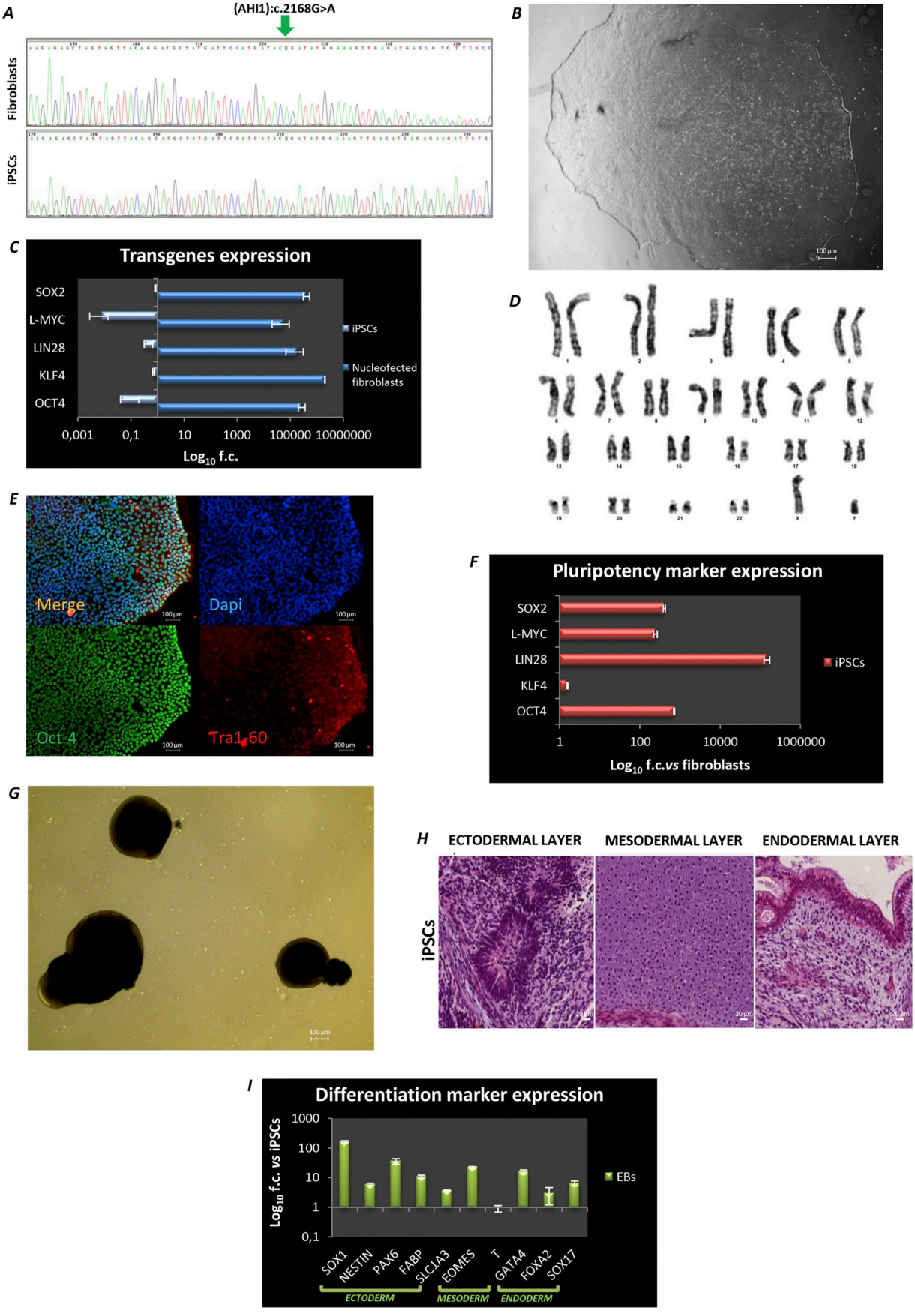

(caption on next page)

Fig. 1. Characterization of CSSi007-A (4383) A. Detection of homozygous mutation: green arrow indicates the mutation site (AHI1):c.2168G > A. B. Phase contrast imaging of the morphology of iPSC line. C. Transgenes expression analysis through qRT-PCR demonstrates the loss of episomal vectors during amplification. D. Cytogenetic analysis showing the normal karyotype of CSSi007-A (4383). E. Representative immunofluorescent stainings showing the expression of stem cell markers such as OCT-4 (green) and TRA-1-60 (red), nuclei was counterstained with DAPI. F. qRT-PCR shows the expression of endogenous stem cell markers in JS iPSCs with respect to fibroblasts used as reference. G. Spontaneous differentiation of JS iPSC in embryoid bodies. H. The injection of iPS cells produced teratoma in vivo. I. Differentation marker expression analysis. Embryoid bodies express the three germ layer markers.

gene, which encodes a cytoplasmic multidomain protein localized in the basal body of the primary cilium, also known as jouberin, composed of an N-terminal coiled-coil domain, WD40 repeats and a C-terminal SH3 domain (Ferland et al., 2004; Valente et al., 2006; Lancaster et al., 2011). The patient presented here, a 27-year old male, was found to carry a homozygous pathogenic missense variant in *AHI1 (c.2168G > A, p. Arg723Gln)*. Skin fibroblasts from the patient were reprogrammed into iPSCs, using three non-integrative episomal vectors containing the reprogramming factors *OCT 3/4, SOX2, L-MYC, KLF4, LIN28, SHP53*. The presence of the disease-related mutation (AHI1): c.2168G > A in fibroblasts was confirmed by Sanger sequencing (Fig. 1A) in the generated iPSCs. JS iPS cell colonies displayed a typical morphology of human pluripotent stem cells and growth behavior (Fig. 1B). We also examined the presence of episomal plasmid DNA in the established iPSCs, using primers specific to a sequence that is common in all three reprogramming plasmids and we observed that after 10 passages the iPSCs were devoid of vector sequences as shown by qRT-qPCR, using, as positive control, the fibroblasts after one week from episomal nucleofection (Fig. 1C). We confirmed the genomic stability of iPSCs through karyotype, which provided a normal diploid 46, XY chromosome arrangement without any detectable abnormalities (Fig. 1D). Staining for endogenous marker TRA-1-60 and OCT-4 demonstrated the pluripotency of these iPSCs (Fig. 1E), that was confirmed through qRT-PCR (Fig. 1F). The *in vitro* spontaneous differentiation potential was demonstrated by the formation of embryoid bodies (EBs) (Fig. 1G) and teratoma formation *in vivo* (Fig. 1H). qRT-PCR analysis showed the endogenous expression of the three germ layers markers (Fig. 1I). PCR-based detection tests confirmed the absence of Mycoplasma contamination at this stage (Supplementary Fig. 1). In addition, Short Tandem Repeat (STR) profiling confirmed that these iPSC lines had the same genetic identity with respect to the donor's fibroblasts (Data available with the authors).

Materials and methods

Skin biopsy and fibroblast reprogramming

The skin biopsy was mechanically processed and maintained in fibroblast medium (DMEM high glucose, 20% FBS, 2mML-glutamine and 1% penicillin–streptomycin (all reagents from Sigma Aldrich)). Subsequently, 1 × 105 fibroblasts were nucleofected with 3 μg 1:1:1 mix of the episomal plasmids pCXLE-hUL (Addgene #27080), pCXLEhSK (Addgene #27078) and pCXLE-hOCT4-shp53 (Addgene #27077). On day 7, the nucleofected fibroblasts were counted, plated on Matrigel (1:100) (BD Biosciences) and cultured in NutristemXF medium (Biological Industries). The emergent hiPSC colonies were picked according to their hESC-like colony morphology and expanded under feeder-free conditions. Absence of mycoplasma contamination was verified using N-Garde Mycoplasma PCR kit (EuroClone) which detects the presence of mycoplasmas in cell culture supernatants by PCR amplification using a reaction mixture containing all the ingredients necessary for PCR, positive control is provided by the kit. 1Kb was used ad ladder in the running. After ten passages, the clearance of the exogenous reprogramming factors was confirmed by qRT-PCR (Table 1).

Embryoid body formation

For the generation of EBs, mechanically detached iPSC were plated in Petri dishes in NutristemXF medium, which was substituted with differentiation medium: DMEM/F12, 20% KOSR (Gibco), 0,1 mM NEAA, 0.1 mM β-mercaptoethanol, 1% Pen/Strep the following day. Fourteen days later, EBs were pelletted and RNAs were extracted for qRT-PCR analysis.

Teratoma formation

Approximately iPSCs from six well plates combined with a Matrigel substrate (Corning, Inc., USA) were injected into the right flank of nude mice. After 1 month, tumors were collected for histological analysis to check for their *in vivo* differentiation capacity into derivatives of all three germ layers.

Real-Time PCR analysis

Total RNAs were extracted using Trizol reagent (Life Technology) and cDNA synthesized using the High capacity cDNA RT (Life Technology) following manufacturer's recommendations. qPCR analysis was performed in three minimum independent biological experiments with TaqMan primers (Table 2) for three germ layers (Thermo Fischer Scientific) and Sybergreen primers (Table 2) for stemness markers according to the manufacturer's protocol. The expression ratio of the target genes was calculated by using the $2^{-\Delta\Delta Ct}$ method, considering 18S as reference gene.

Immunofluorescence staining

Cells were fixed using 4% paraformaldehyde and stained. The cells were incubated with Blocking Buffer (PBS containing 20% Normal Goat Serum, 0.1% Triton X-100) for 30 min at room temperature. Next, primary antibodies, listed in Table 2, diluted in blocking buffer were added and incubated O/N at 4 °C. After extensive washing, Alexa Fluor 594- and/or Alexa Fluor 488-conjugated secondary antibodies were added 1 h at room temperature. Cellular nuclei were counterstained with DAPI. Microphotograps were taken using a Nikon C2 fluorescence microscope and NIS Elements 1.49 software.

Karyotype analysis

Pluripotent cells were cultured in T25 flasks coated with Matrigel in Nutristem medium for 2–3 days. Karyotype analysis of metaphase chromosomes were performed using G-banding. Fifteen metaphases were counted and three karyograms analyzed.

STR analysis

Fibroblasts and iPSCs DNA was extracted by Dneasy blood and tissue kit (QIAGEN). PCR amplification of 19 distinct STRs (D13S252, D13S305, D13S634, D13S800, D13S628, D18S819, D18S535, D18S978, D18S386, D18S390, D21S11, D21S1437, D21S1409, D21S1442, D21S1435, D21S1446, DXS6803, XHPRT, DXS1187) was carried out using the QST*Rplusv2 kit (Elucigene Diagnostics), PCR products were separated on an ABI Prism 3130 DNA sequencer and analyzed by GeneMapper version 4.0 (Applied Biosystems).

Table 1
Characterization and validation.

Classification	Test	Result	Data
Morphology	Photography	*Normal*	Fig. 1B
Phenotype	Immunocytochemistry	*Staining of pluripotency markers: Oct4; Tra-1-60.*	Fig. 1C, E, F
	qRT-PCR	*Expression of pluripotency markers: OCT4, LIN28, L-MYC, KLF4, SOX2*	
Genotype	Karyotype (G-banding) and resolution	*46 XY, Resolution 450–500*	Fig. 1D
Identity	STR analysis	*Tested*	Data available with the authors
Microbiology and virology	Sequencing	*Homozygous mutation*	Fig. 1A
	Mycoplasma	*Mycoplasma tested* by N-Garde Mycoplasma PCR kit (EuroClone) is Negative.	Supplementary Fig. 1
Differentiation potential Morphology	Embryoid body formation and Teratoma formation	*Genes expressed in embryoid bodies: SOX1, NESTIN, PAX6, EOMES, T, GATA4, FOXA2, SOX17* *Proof of three germ layers formation.*	Fig. 1G, H, I
	Photography	*Normal*	Fig. 1B
Phenotype	Immunocytochemistry	*Staining of pluripotency markers: Oct4; Tra-1-60.*	Fig. 1C, E, F
	qRT-PCR	*Expression of pluripotency markers: OCT4, LIN28, L-MYC, KLF4, SOX2*	
Genotype	Karyotype (G-banding) and resolution	*46 XY, Resolution 450–500*	Fig. 1D
Donor screening	HIV 1 + 2 Hepatitis B, Hepatitis C	*N/A*	
Genotype additional info	Blood group genotyping	*N/A*	
	HLA tissue typing	*N/A*	

Table 2
Reagents details.

Antibodies used for immunocytochemistry/flow-citometry

	Antibody	Dilution	Company Cat # and RRID
Pluripotency Markers	*Rabbit anti-OCT4*	*1:100*	*Life technologies (A13998)*
	Mouse anti-TRA-1-60	*1:100*	*Life technologies (411000)*
Secondary antibodies	*anti-Rabbit AlexaFluor 488*	*1:10000*	*Invitrogen (A11034)*
	anti-Mouse AlexaFluor 555	*1:10000*	*Invitrogen (A21422)*

Sybr Green Primers used for qPCR	Target	Forward/Reverse sequence (5′-3′)
Episomal genes	*eOCT4*	*Fwd: CAT TCA AAC TGA GGT AAG GG*
		Rev: TAG CGT AAA AGG AGC AAC ATA G
	eKLF4	*Fwd: CCA CCT CGC CTT ACA CAT GAA GA*
		Rev: TAG CGT AAA AGG AGC AAC ATA G
	eLIN28	*Fwd: AGC CAT ATG GTA GCC TCA TGT CCG C*
		Rev: TAG CGT AAA AGG AGC AAC ATA G
	eL-MYC	*Fwd: GGC TGA GAA GAG GAT GGC TAC*
		Rev: TTT GTT TGA CAG GAG CGA CAA T
	eSOX2	*Fwd: TTC ACA TGT CCC AGC ACT ACC AGA*
		Rev: TTT GTT TGA CAG GAG CGA CAA T
Pluripotency markers	*OCT4*	*Fwd: CCC CAG GGC CCC ATT TTG GTA CC*
		Rev: ACC TCA GTT TGA ATG CAT GGG AGA GC
	LIN28	*Fwd: AGC CAT ATG GTA GCC TCA TGT CCG C*
		Rev: TCA ATT CTG TGC CTC CGG GAG CAG GGT AGG
	L-MYC	*Fwd: GCG AAC CCA AGA CCC AGG CCT GCT CC*
		Rev: CAG GGG GTC TGC TCG CAC CGT GAT G
	SOX2	*Fwd: TTC ACA TGT CCC AGC ACT ACC AGA*
		Rev: TCA CAT GTG TGA GAG GGG CAG TGT GC
House-Keeping Gene	*β-ACTIN*	*Fwd: GGC ATC CTC ACC CTG AAG TA*
		Rev: GGG GTG TTG AAG GTC TCA AA

TaqMan primers used for qPCR	Target	Probe
Differentation markers	*SOX1*	*Hs01057642_s1*
	NESTIN	*Hs04187831_g1*
	PAX6	*Hs00240871_m1*
	T	*Hs00610080_m1*
	EOMES	*Hs00172872_m1*
	GATA4	*Hs00171403_m1*
	FOXA2	*Hs00232764_m1*
	SOX17	*Hs00751752_s1*
	β-ACTIN	*Hs 99999903_m1*

Supplementary data to this article can be found online at https://doi.org/10.1016/j.scr.2019.101480.

Acknowledgements

This work was supported by Italian Ministry of Health, Ricerca Corrente 2018-2019 to JR, ERC Starting Grant StG 260888 and Ricerca Finalizzata grant NET-2013-02356160 to EMV.

References

Ferland, R., Eyaid, W., Collura, R., Tully, L., Hill, R., Al-Nouri, D., Walsh, C., 2004, September. Abnormal cerebellar development and axonal decussation due to mutations in AHI1 in Joubert syndrome. Nat. Genet. 36 (9), 1008–1013.

Lancaster, M., Gopal, D., Kim, J., Saleem, S., Silhavy, J., Louie, C., Gleeson, J., 2011, June. Defective Wnt-dependent cerebellar midline fusion in a mouse model of Joubert syndrome. Nat. Med. 17 (6), 726–731.

Valente, E., Brancati, F., Silhavy, J., Castori, M., Marsh, S., Barrano, G., ... Group., I. J, 2006, March. AHI1 gene mutations cause specific forms of Joubert syndrome-related disorders. Ann. Neurol. 59 (3), 527–534.